Osteoarthritis and Cartilage 27 (2019) 1790–1799

Osteoarthritis and Cartilage

Three-dimensional microstructure of human meniscus posterior horn in health and osteoarthritis

I. Kestilä † * [a], E. Folkesson ‡ § [a], M.A. Finnilä † ||, A. Turkiewicz ‡, P. Önnerfjord §, V. Hughes ‡, J. Tjörnstrand ‡ ¶, M. Englund ‡ # [b], S. Saarakkala † || †† [b]

† *Research Unit of Medical Imaging, Physics and Technology, Faculty of Medicine, University of Oulu, Oulu, Finland*
‡ *Lund University, Faculty of Medicine, Department of Clinical Sciences Lund, Orthopaedics, Clinical Epidemiology Unit, Lund, Sweden*
§ *Lund University, Faculty of Medicine, Department of Clinical Sciences Lund, Rheumatology and Molecular Skeletal Biology, Lund, Sweden*
|| *Medical Research Center, University of Oulu, Oulu, Finland*
¶ *Lund University, Skåne University Hospital, Department of Clinical Sciences Lund, Orthopaedics, Lund, Sweden*
# *Clinical Epidemiology Research and Training Unit, Boston University School of Medicine, Boston, MA, USA*
†† *Department of Diagnostic Radiology, Oulu University Hospital, Oulu, Finland*

ARTICLE INFO

Article history:
Received 5 February 2019
Accepted 3 July 2019

Keywords:
Meniscus
Micro-computed tomography
Histopathological score
Osteoarthritis

SUMMARY

Objective: To develop and perform *ex vivo* 3D imaging of meniscus posterior horn microstructure using micro-computed tomography (μCT), and to compare specimens from healthy references against end-stage osteoarthritis (OA) using conventional section-based histology and qualitative μCT.
Design: We retrieved human medial and lateral menisci from 10 deceased donors without knee OA (healthy references) and medial and lateral menisci from 10 patients having total knee replacement for medial compartment OA. Meniscal posterior horns were dissected and fixed in formalin. One subsection underwent hexamethyldisilazane (HMDS) treatment and μCT imaging. Pauli's histopathological scoring was performed for 3 other subsections. The differences in histopathological scores were estimated using mixed linear regression, resulting in fixed effects estimates for within-knee comparisons and adjusted for age and body mass index for between-subjects comparisons.
Results: 3D visualization with μCT qualitatively revealed similar microstructural changes in the posterior horns as conventional histology. The mean histopathological score was higher for medial menisci from OA knees vs both medial reference menisci (mean difference [95% CI], 3.9 [2.6,5.3]), and lateral menisci from OA knees (3.9 [2.9,5.0]). The scores were similar between lateral menisci from OA knees and lateral reference menisci (0.8 [−0.6,2.2]), and between medial and lateral reference menisci (0.8 [−0.3,1.9]).
Conclusions: HMDS-based μCT protocol allows unique 3D visualization of meniscus microstructures. Posterior horns of medial menisci from medial compartment OA knees had higher histopathological scores than both the lateral posterior horns from the same OA knees and medial reference menisci, suggesting a strong association between meniscus degradation and unicompartmental knee OA.

Introduction

The menisci are crescent-shaped fibrocartilaginous wedges located in the medial and lateral compartments of the knee joint. It is currently well established that menisci have important roles in healthy functioning of the knee joint, including load transmission, joint stabilization, and shock absorption[1–4]. Furthermore, menisci have also been suggested to support joint lubrication, nutrient distribution, and proprioception[5].

Degenerative meniscal lesions are highly prevalent in the general population and are associated with increased risk of

* Address correspondence and reprint requests to: I. Kestilä, Research Unit of Medical Imaging, Physics and Technology, Faculty of Medicine, University of Oulu, POB 5000, FI-90014 Oulu, Finland. Tel.: 358-404129850.
E-mail addresses: iida.kestila@oulu.fi (I. Kestilä), elin.folkesson@med.lu.se (E. Folkesson), mikko.finnila@oulu.fi (M.A. Finnilä), aleksandra.turkiewicz@med.lu.se (A. Turkiewicz), patrik.onnerfjord@med.lu.se (P. Önnerfjord), velocity.hughes@med.lu.se (V. Hughes), jon.tjornstrand@med.lu.se (J. Tjörnstrand), martin.englund@med.lu.se (M. Englund), simo.saarakkala@oulu.fi (S. Saarakkala).
[a] Shared first authorship.
[b] Shared senior authorship.

https://doi.org/10.1016/j.joca.2019.07.003

developing knee osteoarthritis (OA)[6,7]. It has been suggested that such degenerative lesions may begin as proteolytic degradation of the meniscus, leading to a decrease in its tensile strength[8]. This in turn may result in a degenerative meniscal tear due to the inability of the weakened meniscus to resist normal loads and shear stress in the knee joint[8]. On the macromolecular level, previous studies have found that collagen content decreases in the degenerated meniscus, whereas water and proteoglycan contents increase[9,10]. From *in vivo* magnetic resonance imaging (MRI) of human knees, it appears that the degeneration is most commonly found in the posterior horn of the medial meniscus[11], making this zone of particular interest to further studies.

Being able to visualize meniscus microstructure with high resolution in three dimensions (3D) may help us better understand meniscus degeneration, and thus potentially shed light on the "meniscal phenotype" of knee OA. *Ex vivo* micro-computed tomography (μCT) has previously been used sparsely for meniscus imaging[12,13]. With soft tissues such as menisci, contrast enhancement is required in order to distinguish different structures when using conventional desktop μCT. For example, CA4+, Ioxaglate, and freeze-drying have been used in previous studies[12,13]. In our earlier work, we developed a contrast agent free Hexamethyldisilazane (HMDS)-based sample processing protocol for osteochondral samples to enable 3D microstructural imaging and analyses of articular cartilage chondrons with μCT[14]. The protocol also shows potential for 3D quantification of collagen distributions[15].

In this study, we aimed to implement our HMDS-based sample processing protocol for meniscus μCT imaging to allow visualization of human meniscal posterior horn microstructures in 3D. Our objective was to detail and compare histological and qualitative μCT features of posterior horns from both medial and lateral menisci of deceased subjects without known knee OA (referred to as reference) and end-stage medial compartment knee OA patients undergoing total knee replacement (TKR). We hypothesize that there are differences between the posterior horns from the medial OA menisci and reference menisci, and that the posterior horns from lateral menisci from OA patients are similar to reference menisci.

Method

Tissue sample selection

This study was approved by the regional ethical review board at Lund University (Dnr 2015/39 and Dnr 2016/865). From our knee tissue biobank MENIX, previously described by Olsson *et al.*[16], we selected both the medial and lateral menisci from the right knee of 10 deceased adult donors (age 18+ years) (5 men, 5 women) obtained from Skåne University Hospital, Lund, Sweden. Donors included in the study had no known diagnosis of knee OA or rheumatoid arthritis. All menisci were obtained within 48 h postmortem and frozen at −80°C within 2 h of extraction.

From the biobank, we also selected both the medial and lateral menisci from 10 medial compartment knee OA patients (5 men, 5 women) who had a TKR at Trelleborg Hospital, Sweden. All menisci were retrieved and frozen at −80°C within 2 h of extraction and later transported to the biobank in Lund on dry ice for further storage at −80°C. To be classified as having medial compartment OA, the surgeon's Outerbridge classification of knee joint cartilage during surgery was required to be a grade IV (exposed bone) in the medial compartment and grade 0 (normal) or I (softening of cartilage) in the lateral compartment[17]. Further, the surgeon's sketch of the patients' menisci (made on a standardized form) needed to indicate that some of the posterior horns remained for both compartments.

These four groups of menisci; medial and lateral donor menisci, and medial and lateral menisci from medial compartment knee OA patients, will hereafter be referred to as (1) medial^{ref}, (2) lateral^{ref}, (3) medial^{OA}, and (4) lateral^{OA}, respectively.

After thawing the specimens in phosphate buffered saline (PBS), the reference menisci were visually inspected, as we required them to be structurally intact (some minor calcifications were allowed) in order to be accepted for the study. For the medial OA menisci, we further required the menisci to have at least two thirds of the substance of the posterior horn remaining (the inner one third was typically missing). The lateral menisci from TKR patients were typically completely intact at the macroscopic level.

The thawed menisci were divided with a scalpel, somewhat posterior to the mid body, into two parts. The part that we used for this study was the posterior horn (with some part of the body remaining) [Fig. 1 (A)]. A hole (3 mm in diameter) was punched vertically through the central part of the posterior horn (approximately 3–5 mm from the capsular insertion, i.e., in the thicker peripheral part of the meniscus). The cylindrical tissue sample that was extracted, as well as the anterior horn and body of the meniscus, were returned to the biobank for future studies. The posterior horns were then fixed in 4% saline-buffered formaldehyde for a minimum of 11 days, followed by excision of a centrally located section for the μCT protocol [Fig. 1 (B)].

Histological preparation and analyses

From the remaining pieces after excision of the μCT section, we obtained vertical and horizontal slices for histopathological analyses [Fig. 1(B) and (C)]. Before slicing, the fixed samples were further dehydrated with alcohol, cleared with xylene, and embedded in paraffin. Wedge-shaped slices (4 μm thick) were cut from three different locations, perpendicular to the circumferentially oriented collagen bundles (Fig. 1 (B), slices 1, 2 and 3). The remaining paraffin blocks were then melted, and the tissues were reoriented and again embedded in paraffin, followed by cutting of horizontal, 4 μm thick slices (from the inner border of the meniscus to the vascular outer region, at approximately 30° to the tibial plateau) from two different locations (Fig. 1(B) and (C), slices H1 and H2). All slices were stained with hematoxylin and eosin (HE), and Safranin-O–Fast Green (SafO–FG), and subsequently imaged with a digital pathology slide scanner (Aperio AT2, Leica Biosystems, Wetzlar, Germany) using 40× magnification. Histological sample processing, staining, and scoring were performed according to the protocol detailed by Pauli *et al.*[18] with minor modifications in the slice cutting method and chemicals used. The total score in this scoring system ranges between 0 and 18, and can be categorized into the following grades: grade 1 (score 0–4), normal tissue; grade 2 (score 5–9), mild degeneration; grade 3 (score 10–14), moderate degeneration; grade 4 (score 15–18), severe degeneration[18]. The scoring was first performed independently by two blinded graders [IK, EF; inter-observer reliability: ICC (95% confidence interval (CI)) 0.85 (0.67, 0.94) for medial menisci and 0.86 (0.72, 0.94) for lateral menisci]. Subsequently, consensus scoring was done for each sub-score, from which an overall consensus score was calculated for each meniscus section (slices 1–3, including the corresponding horizontal slices). The reliability and repeatability results from the histopathological scoring are presented in the supplementary material (Table S1).

HMDS-based μCT imaging

HMDS-based sample processing was conducted according to our previous work with osteochondral samples[14], with slight modifications in the sample processing durations due to the larger specimens used in the current study. Briefly, the fixed μCT samples were first dehydrated in ascending ethanol concentrations (30%–

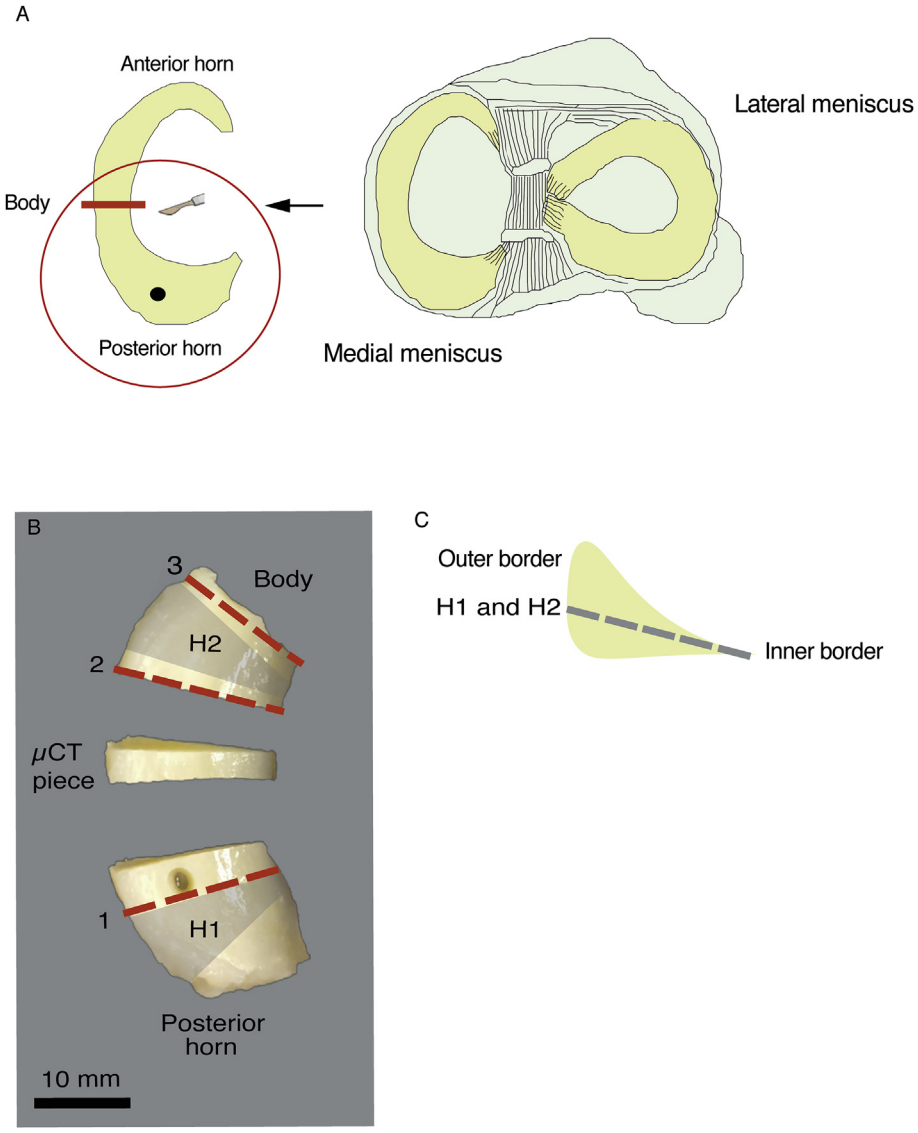

Fig. 1. Sample preparation. A: A schematic illustration of the meniscus posterior horn dissection. B: The locations from where the wedge-shaped histological slices (1, 2, 3), the horizontal histological slices (H1 and H2), and the μCT piece were cut from the meniscus posterior horn. The tissue extracted from the hole next to the slice 1 was reserved for another study. C: A schematic illustration of the plane from which the horizontal histological slices (H1 and H2) are taken.

50%–70%–80%–90%–96%–100%), treated with HMDS for 4 h, and air-dried in a fume hood overnight (details can be found in the supplementary material). Image acquisition was performed using a desktop μCT (SkyScan 1272, Bruker microCT, Kontich, Belgium) with the following settings: tube voltage 40 kV; tube current 250 μA; no additional filtering; isotropic voxel size 2.0 μm; number of projections 2400; averaging 5 frames/projection; and exposure time 1815 ms. NRecon software (v1.6.10.4, Bruker microCT) was used for image reconstruction, during which beam-hardening and ring-artifact corrections were applied. Image rendering was performed with CTVox software (v3.3.0 r1403) provided by the manufacturer.

Statistical analyses

Descriptive data of the histological scores is provided as means and standard deviations (SD) as well as scatterplots. For the statistical analysis, we used linear regression models where the histology scores for each meniscus section were treated as a continuous variable. All analyses were first unadjusted, then adjusted for age, and finally adjusted for age and body mass index (BMI). Data were not adjusted for sex due to the low sample size and the fact that the sample selection had a balanced gender distribution. For comparisons between the groups, a mixed linear regression model was used with the histology score as outcome. The independent variables are group with 4 levels: medial^{OA}, lateral^{OA}, medial^{ref}, lateral^{ref} and meniscus section with 3 levels. We included a random intercept to account for correlation between scores from the same person. We used Satterwhite method for estimation of degrees of freedom and we used *lincom* command in Stata to derive the comparisons of interest from the linear model and their 95% CIs. Even here we used the same method for degrees of freedom. In a sensitivity analysis, we further included an interaction term between the group and meniscus section. We calculated the mean difference in the histology scores between medial^{OA} and medial^{ref}, lateral^{OA} and lateral^{ref}, medial^{OA} and lateral^{OA}, as well as medial^{ref} and lateral^{ref} with 95% CIs. Importantly, as our design was fully balanced (the same number of samples and sections from

each knee and compartment) the above model results in so-called fixed-effect estimates for the within-knee comparisons (i.e. medial^{OA} vs lateral^{OA} and medial^{ref} vs lateral^{ref}). These fixed effects estimates account for all knee-specific confounding factors (both measured and unmeasured). Stata 15 was used for all statistical analyses.

Results

Description of study subjects

The age range of deceased donors (18–77 years, median 50.5) was greater than the TKR patients (51–76 years, median 61.5) (Table I). The TKR patients had a slightly higher median weight than

Table I
Study subjects' characteristics

ID	Sex	Age (at surgery/death)	Height (cm)	Weight (kg)	OA patient/Donor	Knee side
1	Male	72	172	85	OA	Left
2	Female	53	174	68	OA	Left
3	Female	61	156	63	OA	Right
4	Male	65	184	93	OA	Right
5	Female	60	164	79	OA	Left
6	Male	61	186	105	OA	Right
7	Male	68	177	83	OA	Right
8	Female	62	160	78	OA	Right
9	Male	76	172	85	OA	Right
10	Female	51	166	103	OA	Left
11	Male	49	180	107	Donor	Right
12	Female	18	178	52	Donor	Right
13	Male	51	175	82	Donor	Right
14	Female	31	170	66	Donor	Right
15	Female	61	155	56	Donor	Right
16	Male	58	190	120	Donor	Right
17	Female	74	162	67	Donor	Right
18	Female	77	157	55	Donor	Right
19	Male	43	173	127	Donor	Right
20	Male	50	176	106	Donor	Right

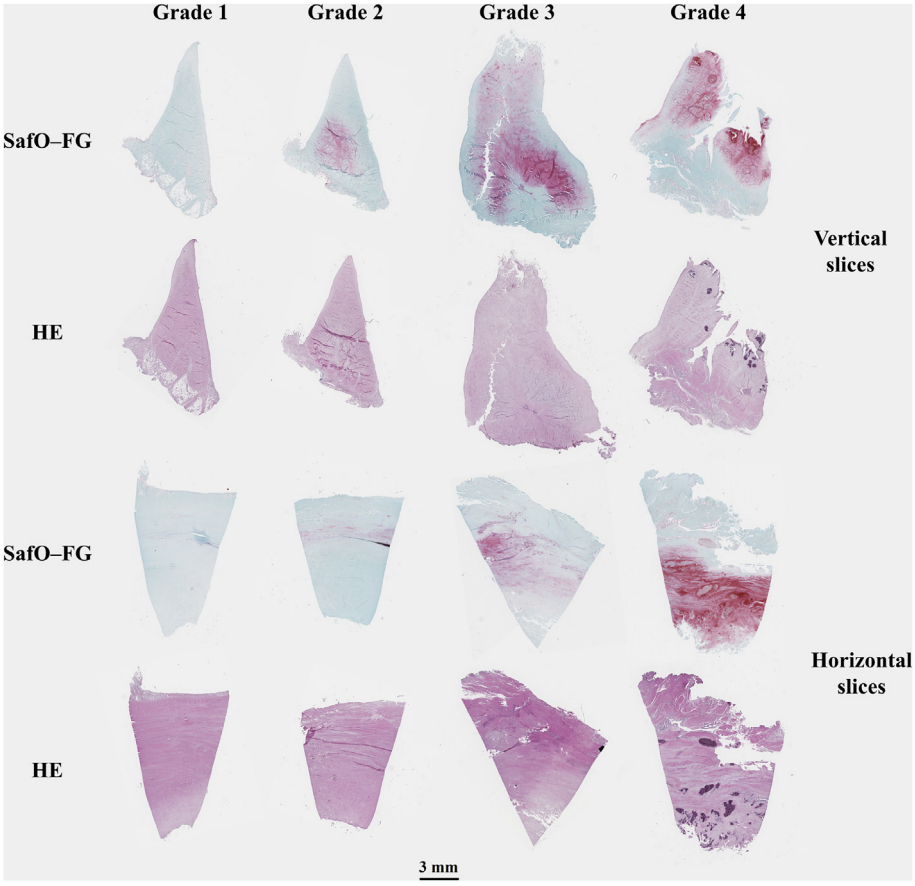

Fig. 2. Histological images from Safranin-O–Fast Green (SafO–FG), and hematoxylin and eosin (HE)-stained vertical and horizontal slices. Representative histological meniscal slices for Pauli's histopathological grades 1–4 were imaged with a digital pathology slide scanner.

the donors, but similar median height (Table I). Table S2 includes more detailed information about the individual study subjects.

Histopathological analyses

Virtual light microscopy images comparing meniscus slices from histopathological grades 1 to 4 revealed that larger histopathological grades were associated with more degenerated meniscus borders, more red staining in the SafO-FG slices, and more disorganized collagen networks in the horizontal slices (Fig. 2). The histopathological consensus scores of each meniscus section used in this study are presented in the supplementary material (Table S2).

HMDS-based μCT imaging

3D visualizations of menisci imaged with HMDS-based μCT showed that samples with larger histopathological grades had more degenerated surfaces and disorganized collagen fibers than those with lower grades (Fig. 3). Furthermore, grade 1–2 menisci appeared smaller than the more degenerated (grade 3–4) menisci (Fig. 3). When comparing μCT images to conventional HE and SafO-FG-stained histological slices (Figs. 2 and 4), several structural features such as surface morphology and collagen network organization, both of which are evaluated in Pauli's scoring system, are also visible in μCT images. Furthermore, meniscus cells, calcifications, channel-like structures penetrating the meniscus from its outer border, and different collagen layers, could be visualized with HMDS-based μCT (Figs. 3 and 4, Supplementary videos S1 and S2). The physical size (width) of samples imaged with the desktop μCT system was limited to 8 mm due to the image resolution used in this study, and thus, some of the largest samples did not fit entirely in the field of view.

Supplementary video related to this article can be found at https://doi.org/10.1016/j.joca.2019.07.003

Reference vs OA menisci

Medial^{OA} menisci had the highest total histopathological consensus scores in all sections, whereas medial^{ref} and lateral^{ref} menisci, and lateral^{OA} menisci had similar scores (except for in section 1, where the lateral^{OA} menisci on average had slightly higher total scores) (Table II). The age range of reference subjects was much wider than in the OA patients, and the total score increased with age (Fig. S1). Moreover, the medial^{OA} menisci were found to have generally higher and less distributed scores than the medial^{ref}, lateral^{ref}, and the lateral^{OA} menisci (Fig. S1). When adjusting for age, and subsequently for age and BMI, there were differences in total scores between the medial^{OA} and medial^{ref} menisci, on average 3.9 (95%CI 2.6, 5.3), as well as between medial^{OA} and lateral^{OA} menisci (3.9 [2.9, 5.0]). In contrast, the lateral^{OA} and lateral^{ref} menisci (0.8 [-0.6, 2.2]), and the medial^{ref} and lateral^{ref} menisci (0.8 [-0.3, 1.9]) had similar scores (Fig. 5, Table S3). In a section-wise analysis (adjusted for age, and then for age and BMI), the medial^{OA} menisci were found to have higher histopathological scores in all three sections compared to the medial^{ref} menisci. When compared to the lateral^{OA} menisci, the medial^{OA} menisci had higher scores in sections 2 and 3 (Fig. 6, Table S4). The largest difference in the total score was observed between the medial^{OA} and lateral^{OA} menisci in section 3 (closest to the body region, 5.5 [3.8, 7.2]). On the other hand, in section 1 (closest to the tip of the posterior horn) the difference in histological scores between these groups was smaller than in the other sections (1.7 [−0.04, 3.4]) (Fig. 6, Table S4). Furthermore, in section 1, the lateral^{OA} menisci had higher scores than the lateral^{ref} menisci (3.7 [1.8, 5.7]). The same was observed between medial^{ref} and lateral^{ref} menisci (2.1 [0.4, 3.8]). The mean (SD) consensus sub-scores of the meniscus sections in the four sample groups are presented in the supplementary material (Table S5).

Discussion

To our knowledge, this study is the first presentation of an HMDS-based sample drying protocol that enables 3D imaging of meniscus microstructures with a conventional desktop μCT. This method enables unique 3D visualization of several features that otherwise can only be seen using 2D histology techniques, which require extensive sample preparation, slicing, and staining. Using the HDMS-based μCT technique and the histopathological analyses, we found that degeneration of the meniscus posterior horn in

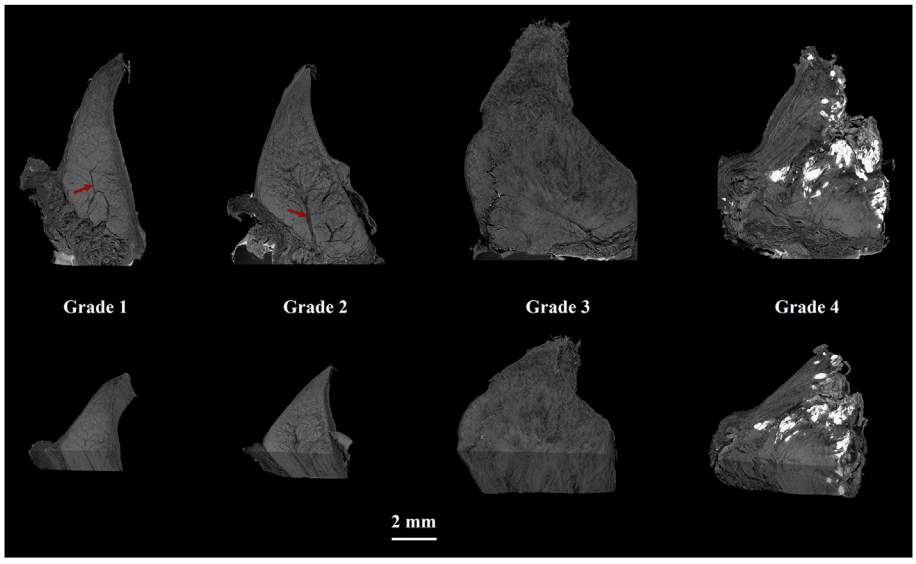

Fig. 3. Volumetric visualizations of μCT images from HMDS-treated meniscal samples representing Pauli's meniscus histopathological grades 1–4. μCT images appear to contain similar microstructural information as needed for Pauli's grading. Channel-like structures were clearly visible especially in the samples with lower grades (red arrows). Ectopic calcification appeared as white areas in the μCT images, and was especially prominent in grade 4 samples.

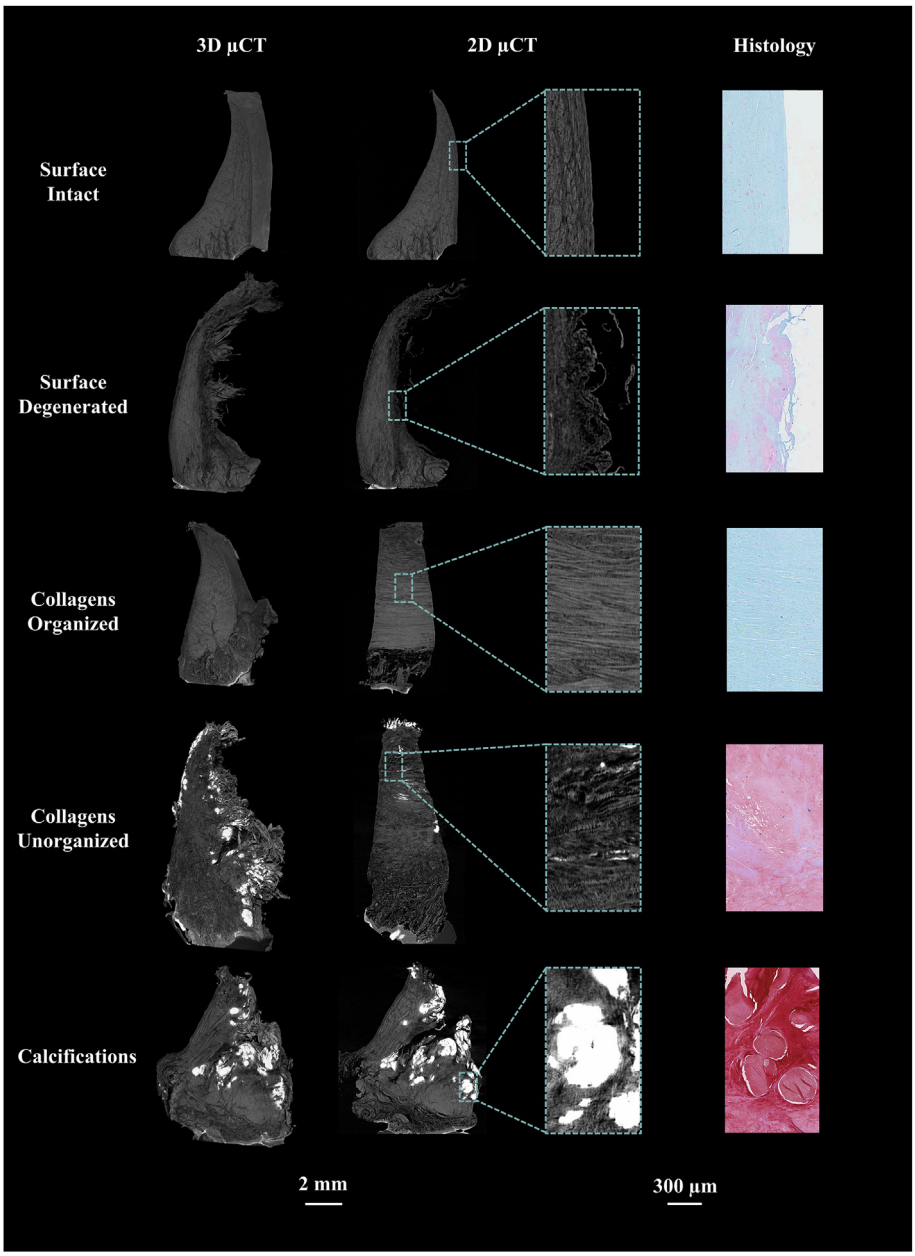

Fig. 4. Representation of different structural features in the meniscus, visible both in µCT and histology.

Table II
Descriptive statistics describing the differences between sample groups and meniscus sections. Results are displayed as means (SD) of the total histopathological (Pauli) score

	$Medial^{OA}$	$Lateral^{OA}$	$Medial^{ref}$	$Lateral^{ref}$
	Mean (SD)	Mean (SD)	Mean (SD)	Mean (SD)
Section 1	14.3 (2.3)	12.6 (2.5)	9.6 (1.8)	7.5 (2.7)
Section 2	14.1 (1.7)	9.5 (2.5)	8.5 (3.5)	8.2 (3.7)
Section 3	14.9 (1.2)	9.4 (1.8)	9.3 (3.0)	9.3 (3.9)

knees from end-stage medial compartment knee OA was mainly present in the medial meniscus, suggesting a strong relationship between the meniscus and the osteoarthritic process in the diseased knee compartment.

The HMDS-based µCT methodology we describe in this study offers several advantages compared to existing methods of tissue imaging. Firstly, it enables volumetric visualization and evaluation of the tissue's 3D organization, therefore giving additional information compared to conventional section-based histology. The technique also offers better resolution than clinical or *ex vivo* MRI at present. Secondly, instead of using external contrast agents such as CA4+ or Ioxaglate, drying the samples using HDMS allows contrast to arise from the tissue itself, and not from the distribution of any specific contrast agent. HMDS was used as a drying agent in our protocol since it is believed to cross-link proteins and therefore stiffen the tissue during the sample processing[19,20]. Thus, the sample appears not to fracture or disintegrate during processing[19,20]. Moreover, in our earlier work, HMDS-based sample drying was shown to enable imaging of the microstructure and chondrons of articular cartilage[14,15], motivating our hypothesis that a similar sample processing protocol should also work with the meniscus.

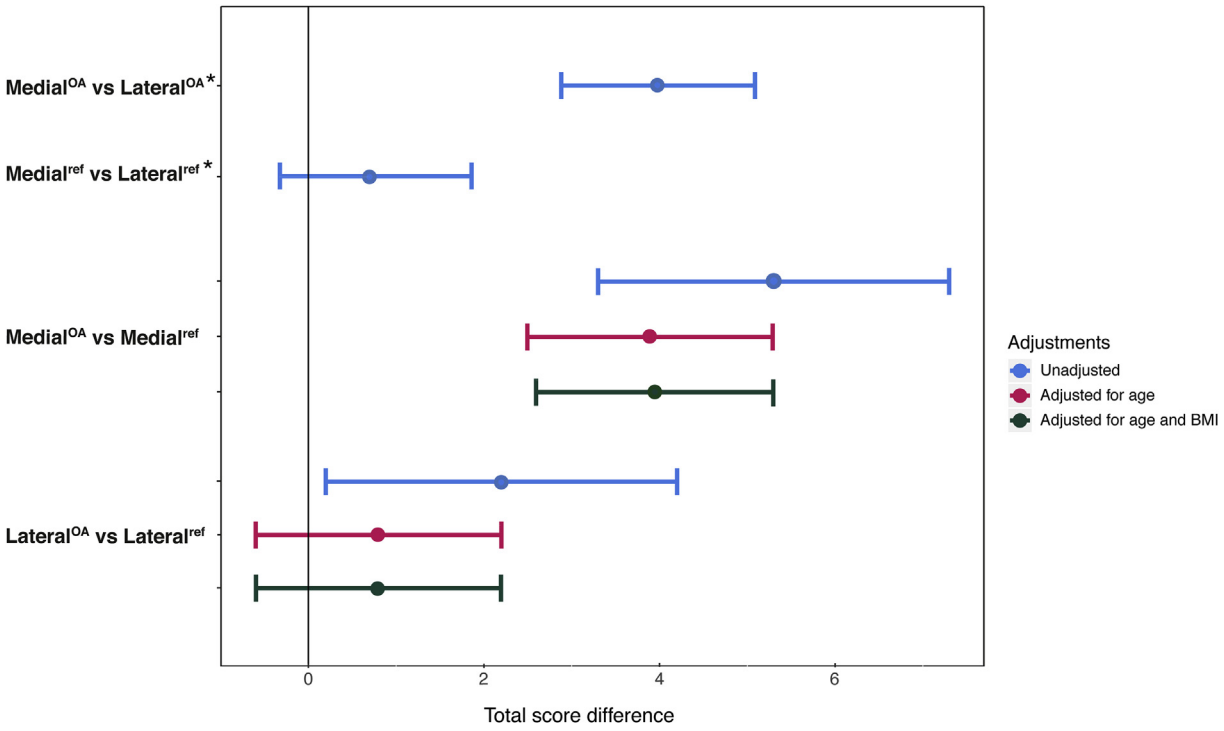

Fig. 5. Comparisons of the posterior horns from medial and lateral reference menisci with posterior horns of medial and lateral menisci from patients with medial compartment knee OA; results show mean difference in total histopathological score (Pauli) with 95% confidence interval. *This comparison was performed between medial and lateral menisci from the same knee, and thus adjusted for all person- and knee level confounding through use of a fixed effects model.

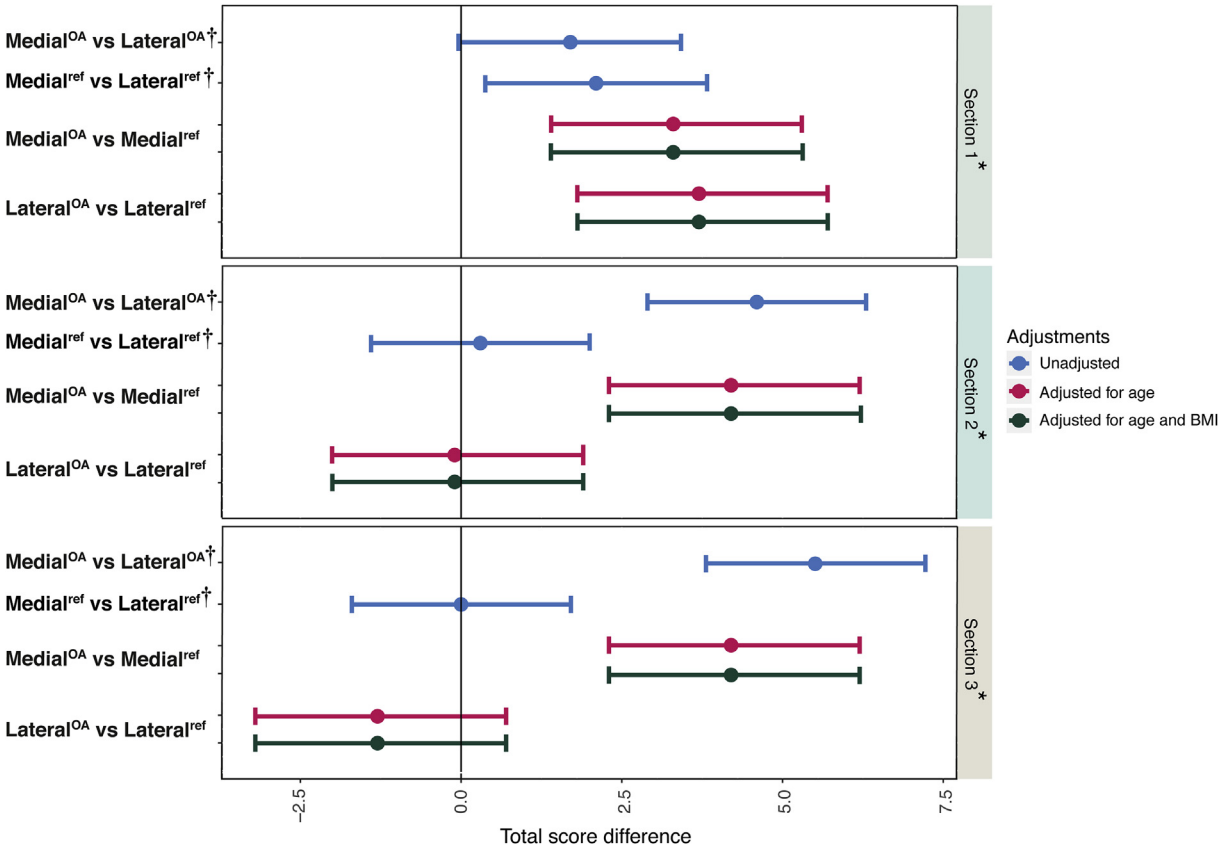

Fig. 6. Mean difference in total histopathological (Pauli) scores displayed with 95% confidence interval in the three sections* (referring to histological slices 1,2 and 3 from the meniscus, see Fig. 1). The model was adjusted for age, and then for age and BMI. †This comparison was performed between medial and lateral menisci from the same knee, and thus adjusted for all person- and knee level confounding through use of a fixed effects model.

From the qualitative μCT analyses that we performed, we found that several structural features visualized with histology, such as surface morphology, collagen organization, and tissue calcifications, were also visible in the μCT images. Moreover, meniscus cells, different collagen layers, and channel-like structures penetrating from the peripheral border of the meniscus were observed (Figs. 3 and 4). These channel-like structures do not significantly attenuate X-rays, and therefore might represent vascularization. However, they appear to penetrate deeper than what has been reported in the literature; vascularization should be limited to the peripheral 10–30% of the meniscus, with increased vascularity in the anterior and posterior horns[5,21]. More likely, the channel-like structures may represent radially oriented tie-fibres that form a branching and sheet-like network wrapping around the circumferentially oriented collagen bundles in the main body of meniscus[22], or loose connective tissue, as described by Petersen *et al.*[23]. Interestingly, Andrews *et al.* reported that blood vessels, surrounded by proteoglycan-rich regions, are enclosed by these tie-fibre sheets[22]. Indeed, we do observe similar branch-like proteoglycan-rich structures in the SafO-FG-stained meniscal histological slices, which appear to coincide with the channel-like structures we observe in μCT. However, in order to fully rule out vascularization and determine the exact origin of these cavities, further histological evaluations with specific stains for neurovascular structures need to be conducted.

From our qualitative μCT analyses, we also observed that more intact menisci (histolopathological grades 1–2) appeared to be smaller in size than the degenerated (grade 3–4) menisci (Fig. 3). This finding is supported by previous MRI studies where OA menisci have been reported to be hypertrophic and often in a subluxated/extruded position in the knee joint[24,25]. One of these studies reported that the meniscus body and posterior horn are thicker in OA menisci, and that the meniscus volume is increased in the entire meniscus in OA knees when compared to non-OA knees[24]. This corresponds well with our qualitative μCT findings. The mechanisms causing meniscal hypertrophy, however, are not completely understood. One possibility is that due to collagen degeneration and tears, the meniscus becomes edematous, in particular if subluxated and located mainly outside of the joint margin, i.e. no longer weight bearing. Meniscal hypertrophy might also be a reparative response to the degeneration caused by OA and failed tissue mechanical properties.

Our section-based histological analyses revealed that medial^{OA} menisci have significantly higher histopathological scores when compared to lateral^{OA} menisci and medial^{ref} menisci. As expected, the lateral^{ref} and medial^{ref} menisci had similar histopathological scores, but it was also observed that the lateral^{OA} and the lateral^{ref} menisci had similar scores. This suggests that the degenerative changes of the meniscal posterior horn that occur in medial compartment knee OA are also localized in the medial side of the joint, and the lateral side remains largely unaffected. When studying three sections from three different regions of the meniscus posterior horn separately, the medial^{OA} menisci showed higher histopathological scores in all three sections compared to the medial^{ref} menisci. Compared to the lateral^{OA} menisci, the medial^{OA} menisci had higher scores in sections 2 and 3. In section 1 (closest to the tip of the posterior horn), the difference in histological scores between the medial^{OA} and the lateral^{OA} menisci was smaller than in the other sections. Furthermore, in section 1, the lateral^{OA} menisci had higher scores than the lateral^{ref} menisci, and the medial^{ref} menisci had higher scores than the lateral^{ref} menisci. This could indicate that the degeneration eventually also may engage the lateral compartment, where it initiates in the tip of the posterior horn. This is also supported by the previous literature where it has been reported that in both medial and lateral compartments, the meniscal degeneration is most commonly found in the posterior horn[11,18]. Moreover, the tip of the posterior horn of medial^{ref} menisci was more degenerated than the corresponding lateral^{ref} menisci, which suggests that the degeneration may initiate close to the tip of the medial posterior horn. Again, this is in line with previous studies showing that in the general population, the degeneration is typically found in the posterior horn of the medial meniscus[11,26].

Age and BMI are strong risk factors for OA and are likely associated with the differences in histopathological scores between the OA and reference groups. Indeed, in the statistical analyses of OA vs reference subjects, we found that adjustment for age decreased the differences in histopathological scores between the groups. However, additional adjustment for BMI had only limited impact on the results.

One major limitation of this work was that the tissue specimens used were first frozen and then thawed before processing and analysis. This, however, was inevitable because sample collection in the biobank in Lund, Sweden was already ongoing before the onset of this study. Nonetheless, all samples in this study underwent the same sample-preparation processes, and the results of the present study should thus still be comparable to each other. Another limitation is that even though HMDS has been shown to be a suitable drying agent that preserves the microstructure of osteochondral samples[14], it should be taken into account that the tissue structure in HDMS-dried meniscal samples may not resemble its intact state *in vivo*. Although this protocol is applicable to any laboratory with access to a μCT scanner, it is important to notice that this methodology is not suitable for *in vivo* experiments as drying the tissues in living animals/patients is not feasible and safe by any means. Drying the sample, however, makes the tissue stable and allows μCT imaging of its microstructure with high resolution. A third limitation is that μCT, like other imaging modalities, has some artifacts, such as streaking and ring artifacts. Most significantly for this study, the calcifications in the menisci cause streaking artifacts, which occur due to substantial differences in X-ray attenuation between the calcified and non-calcified meniscus regions. These artifacts could be prevented by decalcifying the samples during sample processing. However, on the other hand, doing so might make the calcifications less visible in the μCT images, which would not be a true reflection of the structural state. The different age distributions between the reference group and the medial compartment knee OA patients in the study were also a concern. However, these differences were taken into account via multivariable modelling.

To summarize, in this study we implemented an HMDS-based sample processing protocol for visualizing human *ex vivo* meniscus microstructures in 3D using a desktop μCT for the first time. When compared to adjacent 2D histological sections, similar structural features, such as surface morphology, collagen organization, and calcifications could be visualized in 3D with μCT. This method enables visualization of considerably larger volumes and evaluation of the tissue's volumetric organization. When compared to conventional section-based histology, the method may provide additional important 3D information regarding the early degenerative changes in the meniscus during OA. Moreover, this study also found that medial OA menisci had much higher histopathological scores than both medial reference menisci, as well as lateral menisci from within the same knees, suggesting a strong relationship between meniscus degradation and unicompartmental knee OA.

Author contributions

Conception and design: IK, EF, SS and ME.
Provision of study materials and tissue preparation: ME, EF, VH, PÖ, JT, IK, MF, SS and IK.
Micro-CT imaging: IK and MF.
Histology assessment: IK and EF.
Statistical analysis: IK, EF, AT.
Interpretation of results: All coauthors.
Drafting of the article: IK and EF.
Critical revision of the article for important intellectual content: MF, AT, PÖ, VH, JT, ME and SS.
Final approval of the article: All coauthors.

Competing interest statement

- AT works as an associate editor (statistics) in Osteoarthritis and Cartilage.
- PÖ has received grants from Greta and Johan Kock Foundation, the Swedish Rheumatism Association, the Crafoord Foundations, the Österlund Foundation, the Foundation Olle Engkvist Byggmästare, and the Faculty of Medicine, Lund University, Sweden.
- ME has received grants from European Research Council, the Swedish Research Council, the Foundation for Research in Rheumatology, the Greta and Johan Kock Foundation, the Swedish Rheumatism Association, the Österlund Foundation, the Governmental Funding of Clinical Research program within the National Health Service in Sweden, and the Faculty of Medicine, Lund University, Sweden.
- SS has received grants from European Research Council, Academy of Finland, and Foundation for Research in Rheumatology, and has one pending patent application (University of Oulu).
- Other authors (IK, EF, MF, VH, and JT) report no conflicts of interest.

Declaration of funding

This project has received funding from the European Research Council (ERC) under the European Union's Horizon 2020 research and innovation programme (grant agreement No 771121) and European Research Council under the European Union's Seventh Framework Programme (FP/2007–2013) (grant agreement No 336267). This work was also supported by the Swedish Research Council (Dnr 2014–2348), the Foundation for Research in Rheumatology (FOREUM) (018EnglundPreCl), the Greta and Johan Kock Foundation, the Swedish Rheumatism Association, the Österlund Foundation, the Governmental Funding of Clinical Research program within the National Health Service (ALF) in Sweden, and the Faculty of Medicine, Lund University, Sweden.

Role of the funding source

The funders had no role in study design, data collection and analysis, decision to publish, or preparation of the manuscript.

Acknowledgements

We would like to thank the MENIX clinical staff at Trelleborg Hospital, the Tissue Donor Bank at Skåne University Hospital, and the Department of Forensic Medicine in Lund for their grateful collaboration that enabled sample collection. We would also like to acknowledge Ms. Tarja Huhta, Laboratory Technician, for preparatory work with the histological samples.

Supplementary data

Supplementary data to this article can be found online at https://doi.org/10.1016/j.joca.2019.07.003.

References

1. Seedhom BB, Hargreaves DJ. Transmission of the load in the knee joint with special reference to the role of the menisci: PartII: experimental results, discussion and conclusion. Eng Med 1979;8:220–8.
2. Shoemaker SC, Markolf KL. The role of the meniscus in the anterior-posterior stability of the loaded anterior cruciate-deficient knee. Effects of partial versus total excision. J Bone Joint Surg Am 1986;68:71–9.
3. Voloshin AS, Wosk J. Shock absorption of meniscectomized and painful knees: a comparative in vivo study. J Biomed Eng 1983;5:157–61.
4. Seitz AM, Wächter L, Ignatius A, Dürselen L. The Shock-Absorbing News about Meniscus 2019. ORS 2019 Annual Meeting Paper No. 0267.
5. Fox AJS, Wanivenhaus F, Burge AJ, Warren RF, Rodeo SA. The human meniscus: a review of anatomy, function, injury, and advances in treatment. Clin Anat 2015;28:269–87.
6. Noble J, Hamblen DL. The pathology of the degenerate meniscus lesion. J Bone Joint Surg Br 1975;57:180–6.
7. Englund M, Roos EM, Lohmander LS. Impact of type of meniscal tear on radiographic and symptomatic knee osteoarthritis: a sixteen-year followup of meniscectomy with matched controls. Arthritis Rheum 2003;48:2178–87, https://doi.org/10.1002/art.11088.
8. Englund M, Guermazi A, Lohmander SL. The role of the meniscus in knee osteoarthritis: a cause or consequence? Radiol Clin N Am 2009;47:703–12.
9. Herwig J, Egner E, Buddecke E. Chemical changes of human knee joint menisci in various stages of degeneration. AnnRheumDis 1984;43:635–40.
10. Adams ME, Billingham ME, Muir H. The glycosaminoglycans in menisci in experimental and natural osteoarthritis. Arthritis Rheum 1983;26:69–76.
11. Englund M, Guermazi A, Gale D, Hunter DJ, Aliabadi P, Clancy M, *et al*. Incidental meniscal findings on knee MRI in middle-aged and elderly persons. NEnglJMed 2008;359:1108–15, https://doi.org/10.1056/NEJMoa0800777.
12. Lakin BA, Grasso DJ, Stewart RC, Freedman JD, Snyder BD, Grinstaff MW. Contrast enhanced CT attenuation correlates with the GAG content of bovine meniscus. JOrthopRes 2013;31:1765–71, https://doi.org/10.1002/jor.22421.
13. Pereira H, Caridade SG, Frias AM, Silva-Correia J, Pereira DR, Cengiz IF, *et al*. Biomechanical and cellular segmental characterization of human meniscus: building the basis for Tissue Engineering therapies. Osteoarthr Cartil 2014;22:1271–81, https://doi.org/10.1016/j.joca.2014.07.001.
14. Kestila I, Thevenot J, Finnila MA, Karhula SS, Hadjab I, Kauppinen S, *et al*. In vitro method for 3D morphometry of human articular cartilage chondrons based on micro-computed tomography. Osteoarthr Cartil 2018;26:1118–26. S1063-4584(18)31281-0 [pii].
15. Rieppo L, Karhula SS, Thevenot J, Hadjab I, Quenneville E, Garon M, *et al*. Determination of extracellular matrix orientation of articular cartilage in 3D using micro-computed tomography. Osteoarthr Cartil 2017;25:S254.
16. Olsson E, Folkesson E, Peterson P, Önnerfjord P, Tjörnstrand J, Hughes HV, *et al*. Ultra-high field magnetic resonance imaging parameter mapping in the posterior horn of ex vivo human

menisci. Osteoarthr Cartil 2019;27:476–83. S1063-4584(18)31556-5 [pii].
17. Outerbridge RE. The etiology of chondromalacia patellae. J Bone Joint Surg Br 1961;43 B:752–7.
18. Pauli C, Grogan SP, Patil S, Otsuki S, Hasegawa A, Koziol J, *et al*. Macroscopic and histopathologic analysis of human knee menisci in aging and osteoarthritis. Osteoarthr Cartil 2011;19:1132–41, https://doi.org/10.1016/j.joca.2011.05.008.
19. Nation JL. A new method using hexamethyldisilazane for preparation of soft insect tissues for scanning electron microscopy. Stain Technol 1983;58:347–51.
20. Lee JT, Chow KL. SEM sample preparation for cells on 3D scaffolds by freeze-drying and HMDS. Scanning 2012;34:12–25, https://doi.org/10.1002/sca.20271.
21. Danzig L, Resnick D, Gonsalves M, Akeson WH. Blood supply to the normal and abnormal menisci of the human knee. ClinOrthopRelatRes 1983;(172):271–6.
22. Andrews SHJ, Rattner JB, Abusara Z, Adesida A, Shrive NG, Ronsky JL. Tie-fibre structure and organization in the knee menisci. J Anat 2014;224:531–7, https://doi.org/10.1111/joa.12170.
23. Petersen W, Tillmann B. Collagenous fibril texture of the human knee joint menisci. AnatEmbryol(Berl) 1998;197:317–24.
24. Wirth W, Frobell RB, Souza RB, Li X, Wyman BT, Le Graverand MP, *et al*. A three-dimensional quantitative method to measure meniscus shape, position, and signal intensity using MR images: a pilot study and preliminary results in knee osteoarthritis. MagnResonMed 2010;63:1162–71, https://doi.org/10.1002/mrm.22380.
25. Jung KA, Lee SC, Hwang SH, Yang KH, Kim DH, Sohn JH, *et al*. High frequency of meniscal hypertrophy in persons with advanced varus knee osteoarthritis. RheumatolInt 2010;30:1325–33, https://doi.org/10.1007/s00296-009-1153-7.
26. Smillie IS. The current pattern of internal derangements of the knee joint relative to the menisci. ClinOrthopRelatRes 1967;51:117–22.